Molecular Therapy
Oncolytics
Original Article

AMERICAN SOCIETY of GENE & CELL THERAPY

Combination of IAP Antagonists and TNF-α-Armed Oncolytic Viruses Induce Tumor Vascular Shutdown and Tumor Regression

Shawn T. Beug,[1,2,3] Stephanie J. Pichette,[1,2,3] Martine St-Jean,[1] Janelle Holbrook,[1] Danielle E. Walker,[1] Eric C. LaCasse,[1] and Robert G. Korneluk[1,2]

[1]Apoptosis Research Center, Children's Hospital of Eastern Ontario Research Institute, Ottawa, ON, Canada; [2]Department of Biochemistry, Microbiology and Immunology, University of Ottawa, ON, Canada

Smac mimetic compounds (SMCs) are anti-cancer drugs that antagonize Inhibitor of Apoptosis proteins, which consequently sensitize cancer cells to death in the presence of proinflammatory ligands such as tumor necrosis factor alpha (TNF-α). SMCs synergize with the attenuated oncolytic vesicular stomatitis virus (VSVΔ51) by eliciting an innate immune response, which is dependent on the endogenous production of TNF-α and type I interferon. To improve on this SMC-mediated synergistic response, we generated TNF-α-armed VSVΔ51 to produce elevated levels of this death ligand. Due to ectopic expression of TNF-α from infected cells, a lower viral dose of TNF-α-armed VSVΔ51 combined with treatment of the SMC LCL161 was sufficient to improve the survival rate compared to LCL161 and unarmed VSVΔ51 co-therapy. This improved response is attributed to a bystander effect whereby the spread of TNF-α from infected cells leads to the death of uninfected cells in the presence of LCL161. In addition, the treatments induced vascular collapse in solid tumors with a concomitant increase of tumor cell death, revealing another mechanism by which cytokine-armed VSVΔ51 in combination with LCL161 can kill tumor cells. Our studies demonstrate the potential for cytokine-engineered oncolytic virus and SMCs as a new combination immunotherapy for cancer treatment.

INTRODUCTION

Smac mimetic compounds (SMCs) are small-molecule drugs designed to imitate the role of the proapoptotic protein, second mitochondria-derived activator of caspases (SMAC). SMCs, such as LCL161, are currently undergoing early phase clinical trials for cancer treatment.[1,2] SMCs function by binding and degrading two key cellular Inhibitors of Apoptosis (IAPs) proteins, cIAP1 and cIAP2. Both cIAP1 and cIAP2 inhibit programmed cell death by suppressing the formation of a ripoptosome-containing death complex.[3,4] In the presence of SMCs, the cIAPs are degraded by the proteasome, resulting in sensitization of cancer cells to tumor necrosis factor alpha (TNF-α)-mediated cell death.[5–7]

We and others have previously shown that SMCs synergize with innate immunostimulants, which in turn trigger the production of endogenous proinflammatory ligands such as TNF-α.[8–11] For instance, SMC treatment is potentiated by infection of an attenuated oncolytic vesicular stomatitis virus (VSVΔ51), an effect that is dependent on the presence of TNF-α, TNF-related apoptosis inducing ligand (TRAIL), and interferon-beta (IFNβ).[8] The use of combination immunotherapies that potentiate SMC treatment poses a very promising approach. However, methods to safely and effectively provide an exogenous source of death ligand without causing adverse effects still need to be developed.

TNF-α was initially proposed to be an attractive therapy given its specific anti-tumor activity and its ability to damage the neovasculature of developing tumors.[12–15] However, the administration of exogenous recombinant TNF-α for cancer treatment to patients was found to cause systemic toxicity and display limited efficacy, hindering the initial promise of TNF-α to be used as a cancer therapeutic.[16,17] Currently, the delivery of recombinant TNF-α is restricted to the setting of isolated limb perfusion for melanoma or sarcoma in combination with melphalan.[18–20] Other efforts have focused on the design of vectors that can deliver the proinflammatory cytokine locally and thereby circumvent the unwanted cytotoxic effects of systemic high-dose TNF-α administration. Recently, the use of viruses has been explored as tools for delivering cytokines locally to cancer cells, such as TNF-α.[21,22] The oncolytic virus (OV) VSVΔ51 has been attenuated in its ability to antagonize the host IFNβ-mediated anti-viral response, and consequently is able to preferentially replicate in cancer cells that contain defects in IFNβ-signaling pathways.[23] Furthermore, the release of IFNβ from infected cells induces a storm of proinflammatory cytokines, activating immune effector cells and triggering anti-viral and –tumor-immune responses.[24] These properties support the rationale that OVs could be engineered to express cytokines in order to enhance an anti-tumor response from the host.[24–32]

Received 26 May 2018; accepted 16 June 2018;
https://doi.org/10.1016/j.omto.2018.06.002.

[3]These authors contributed equally to this work.

Correspondence: Robert G. Korneluk, Apoptosis Research Center, Children's Hospital of Eastern Ontario Research Institute, Ottawa, ON, Canada.
E-mail: bob@arc.cheo.ca

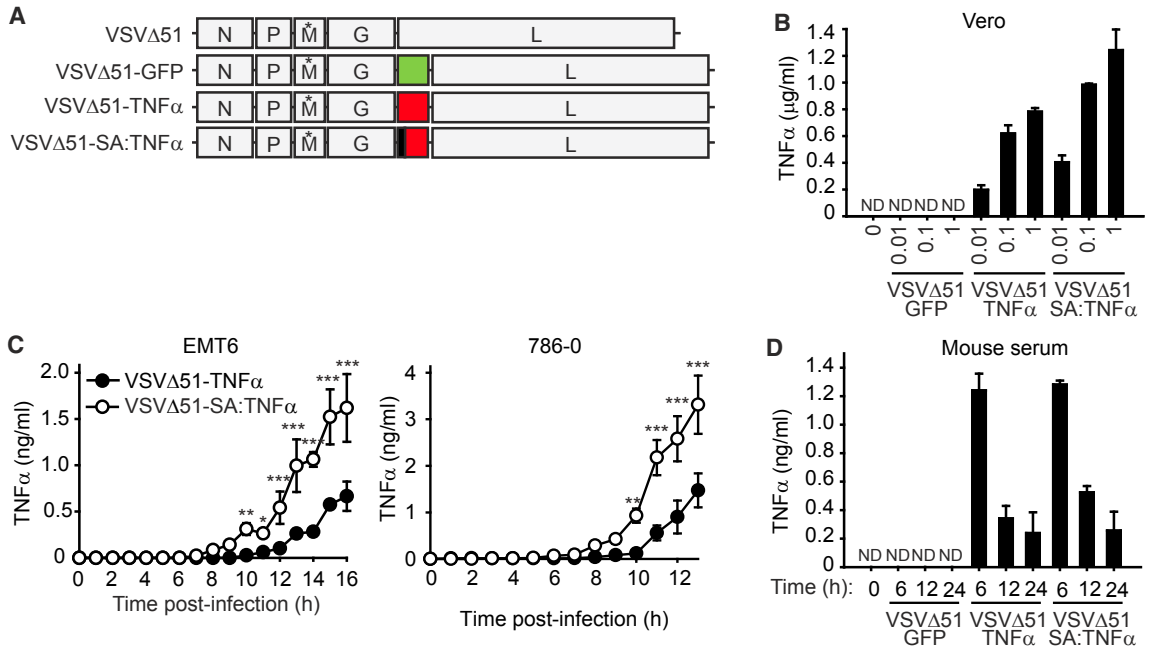

Figure 1. Production of TNF-α from Cells Infected with TNF-α-Armed Oncolytic VSV

(A) Schematic representation of the VSVΔ51 constructs. Green represents GFP, yellow represents TNF-α, and black represents replacement of the membrane anchor domain with the serum albumin (SA) signal peptide sequence. (*) denotes the deletion of the 51st amino acid in the M protein. (B) TNF-α levels were determined by ELISA from supernatants of Vero cells infected with indicated MOI of virus for 16 hr. ND, not detected. Mean, SD. (C) TNF-α levels were detected by ELISA from supernatants of cells infected with 1 MOI of the indicated virus. Two-way ANOVA with Sidak's multiple comparison test: *$p < 0.05$; **$p < 0.01$; ***$p < 0.001$. Mean, SD. (D) Measurement of human TNF-α from mouse serum at the indicated post-infection times. Viruses were delivered i.v. at 1×10^7 PFU virus. Mean, SD.

Given the known synergy between SMC and TNF-α, we reasoned that the generation of an OV vector capable of secreting TNF-α would lead to an enhanced anti-cancer response. The virally derived expression of TNF-α could improve SMC efficacy by eliciting a greater degree of bystander cell killing while minimizing systemic TNF-α-mediated adverse toxic effects. In addition, the treatment with IAP antagonists can induce TNF-α production via the nuclear factor κB (NF-κB) pathway, leading to collapse of the tumor vasculature and thereby inducing a greater degree of tumor cell death. Therefore, the use of SMCs in combination with TNF-α-armed VSVΔ51 could induce a dual mechanism of cancer cell killing through IAP antagonism and neovascular collapse.

RESULTS

TNF-α Is Secreted from Cells Infected with TNF-α-Armed Oncolytic VSV

The VSVΔ51-TNF-α construct that contains an M51 amino acid deletion in the matrix (M) gene was generated by cloning full-length TNF-α between the G and L VSV genes (Figure 1A). We also generated a version of TNF-α whereby the membrane-anchor domain of TNF-α was replaced with the secretory signal peptide of human serum albumin (VSVΔ51-SA:TNF-α). To assess whether TNF-α is efficiently secreted in infected cells, we measured the level of TNF-α in tissue culture supernatants from an OV-permissible cell line. We observed that both TNF-α-armed VSVs secrete TNF-α in a dose-response manner in Vero cells (Figure 1B). As expected, we did not observe elevated levels of TNF-α in Vero cells infected with VSVΔ51-GFP. As we noted that there was an elevated level of detectable TNF-α from VSVΔ51-SA:TNF-α compared to VSVΔ51-SA:TNF-α, we next analyzed whether there is a difference in the kinetics of TNF-α secretion between the two TNF-α-armed OVs. Consistent with the replacement of the membrane-anchor domain with the SA constitutive secretory signal sequence, we observed a higher rate of TNF-α secretion with VSVΔ51-SA:TNF-α (Figure 1C).

Based on these *in vitro* observations, we asked whether we can detect higher levels of TNF-α from administration in mice of VSVΔ51-SA:TNF-α when compared to VSVΔ51-TNF-α. We observed an elevated level of human TNF-α from each TNF-α-armed OV within 6 hr post-infection and that TNF-α levels decreased over a span of 24 hr (Figure 1D). Surprisingly, we did not observe a difference of the amount of TNF-α between the two TNF-α-armed OVs. In addition, we found that the level of endogenous TNF-α was similar in mice infected with either TNF-α-armed virus compared to VSVΔ51-GFP (Figure S1).

SMC Treatment Does Not Impair TNF-α Expression, Viral Kinetics, or Anti-viral Responses

We next determined whether chemical IAP antagonism can affect the secretion of TNF-α in cells infected with TNF-α-armed oncolytic

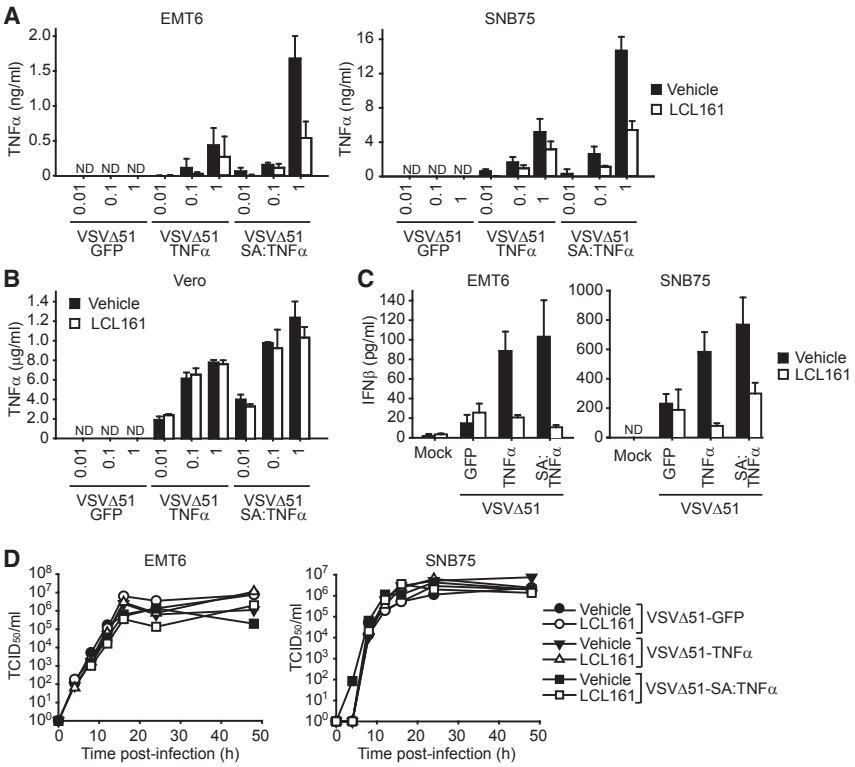

Figure 2. The Combination of TNF-α-Armed Oncolytic VSV and SMC Does Not Impair the Anti-viral Response

(A and B) Detection of TNF-α by ELISA from supernatants of EMT6 and SNB75 (A) or Vero (B) cells treated with vehicle or 5 μM of the SMC LCL161 and the indicated MOI of virus for 16 hr. Mean, SD. (C) IFNβ levels were detected from the supernatant of EMT6 or SNB75 cells treated with vehicle or 5 μM LCL161 and 1 MOI of the indicated virus for 24 hr. Mean, SD. (D) Supernatants from EMT6 or SNB75 cells treated with vehicle or 5 μM LCL161 and 0.1 MOI of the indicated virus were applied to BHK-21 or Vero cells for 48 hr, respectively. Wells with dead cells were scored to calculate the virus titer as $TCID_{50}$/mL.

VSV. We observed that the amount of TNF-α detected in the cell culture supernatants from infected mouse EMT6 or human SNB75 cancer cells were significantly less in the presence of the SMC LCL161 (Figure 2A). However, as EMT6 and SNB75 cells are killed with LCL161 and TNF-α co-treatment,[8] we reasoned that the decrease of TNF-α production is a consequence of cell death induced by SMCs in the presence of TNF-α (Figure S2). Accordingly, we examined the levels of TNF-α from infected Vero cells, which are not sensitive to LCL161 and TNF-α combinatorial treatment (Figure S3) and also lack a functional anti-viral response that limits oncolytic VSV replication and spread. There was no difference in the level of TNF-α detected in the supernatants of Vero cells treated with vehicle or LCL161 treatment and infected with VSVΔ51-TNF-α or VSVΔ51-SA:TNF-α (Figure 2B).

Due to the ability of cIAP1 and cIAP2 to regulate NF-κB signaling, alterations in the protein levels of cIAP1/2 can affect immune responses, including anti-viral signaling mediated by type I IFNs.[33,34] Hence, we explored whether SMC treatment in the presence of exogenous TNF-α impairs the ability of infected cancer cells to elicit an anti-viral response. Consistent with a previous report,[8] we did not detect a difference of IFNβ secretion in EMT6 or SNB75 cells infected with VSVΔ51-GFP and treated with LCL161 (Figure 2C). Strikingly, we observed an elevated level of IFNβ with infection by TNF-α-armed viruses and that LCL161 treatment reduced IFNβ secretion to the same level as VSVΔ51-GFP. However, despite the differences in IFNβ production, there was no difference of virus infectivity or spread as measured by multistep growth curves in EMT6 and SNB75 cells (Figure 2D; Figure S4). Collectively, these results indicate that SMC treatment does not inhibit the production of virally derived TNF-α nor blunt the anti-viral response.

TNF-α-Armed Oncolytic VSV Potently Synergizes with SMC to Induce Apoptosis in Cancer Cells

We next investigated whether the TNF-α-armed OVs improve the ability of SMCs to kill cancer cells. Kill curves performed on LCL161-treated EMT6 and SNB75 cells showed that VSVΔ51-TNF-α and VSVΔ51-SA:TNF-α led to a one-log increase of cell death compared to VSVΔ51-GFP, while leaving normal human fibroblasts (GM38) unaffected (Figure 3A). We also observed increased potency of LCL161-mediated killing in other SMC susceptible cancer cell lines (e.g., CT-26 and 786-0), and in some cases, the oncolytic properties of VSVΔ51 was enhanced with the inclusion of TNF-α (SF539) (Figure S5). On the other hand, we did not observe synergy with TNF-α-armed oncolytic VSV in combination with LCL161 to induce the death of SMC-resistant lung cancer H460 and H661 cells (Figure S5), a property that is due to the presence of the caspase-8 inhibitor, cFLIP.[35]

We also assessed cytotoxicity and apoptosis induction via live microscopy using a caspase-3/7 fluorescent substrate. The combination of LCL161 and VSVΔ51-TNF-α or VSVΔ51-SA:TNF-α lead to a significantly higher rate of cell death compared to VSVΔ51-firefly luciferase (Fluc) (Figure 3B). The elevated kinetics of cancer cell death with the combination of SMC and TNF-α-armed oncolytic VSV may be the cause for decreased TNF-α and type I IFN (Figures 2A and 2C), as there would be less-viable cells the production of anti-viral and proinflammatory factors. As the majority of cancer cells undergoing cell death were positive for active caspase-3/7, we next assessed whether the cells were undergoing death through the extrinsic apoptotic pathway. The engagement of cancer cell death through the TNF-α and TNF-R1 (TNF receptor 1) is dependent on the formation of a death-inducing complex called the ripoptosome. The

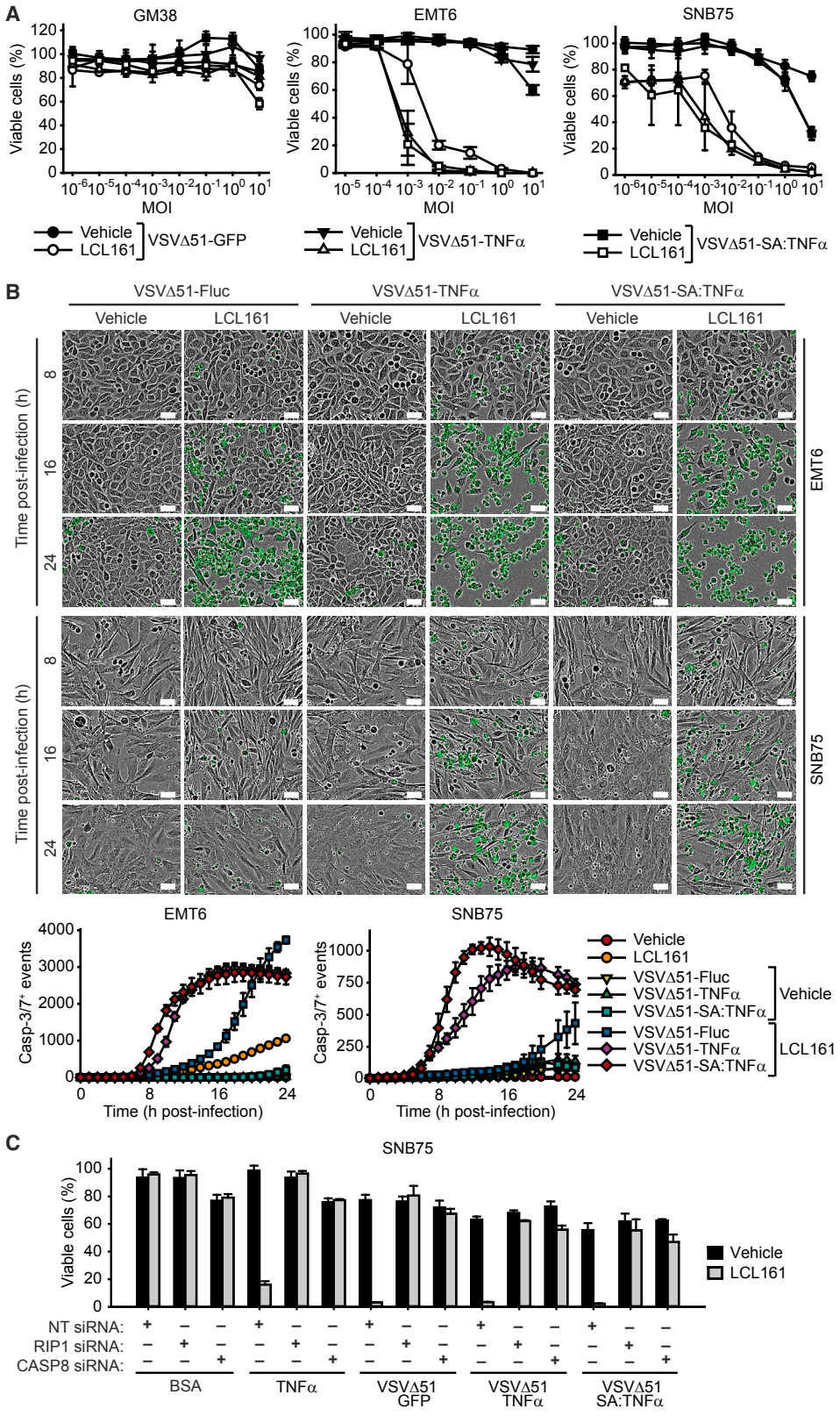

(legend on next page)

silencing of the obligate components Receptor Interacting Protein 1 (RIP1) or caspase-8 completely rescued cancer cell death upon treatment with LCL161 and infection with oncolytic VSV (Figure 3C; Figure S6A), confirming that the cytotoxicity induced by the combinatorial treatment is through apoptosis.

A Combination of SMCs with TNF-α-Armed Oncolytic VSVs Leads to Bystander Cancer Cell Death

In addition to virally derived production of TNF-α, OV infection induces the expression of a plethora of soluble factors that can contribute toward SMC-mediated death of cancer cells.[36] To further characterize the synergistic response, we assessed for bystander cell death using an agarose overlay assay that restricts the spread of virus to adjacent cells but permits the diffusion of secretory proteins to neighboring cells. As anticipated, we observed an increase of cytotoxicity with the combination of LCL161 and VSVΔ51-GFP in EMT6 cells, and the degree of cytotoxicity was enhanced with full-length TNF-α- and SA:TNF-α-armed VSVΔ51 (Figure 4A), indicating that these cytokine-armed viruses are releasing soluble factors that aid in SMC-mediated killing of neighboring uninfected cells. We also conducted this assay in murine CT-26 cells, which are similarly resistant to oncolytic VSV cytotoxicity but are not as sensitive to SMC and TNF-α co-treatment as SNB75 or EMT6 cells. Notably, we did not observe synergy with LCL161 and VSVΔ51-GFP, however, the combination of LCL161 and VSVΔ51-TNF-α or VSVΔ51-SA:TNF-α resulted in a greater degree of cytotoxicity.

To provide additional evidence that the release of soluble factors is responsible for the death of cancer cells in the presence of SMCs, we performed conditioned media transfer assays. Cells were infected with the indicated virus, the supernatant was exposed to UV light to inactivate infectious virions, and then the supernatant was re-applied to virus-naive vehicle- or SMC-treated cells. The application of conditioned media from cells infected with TNF-α-armed OVs onto LCL161-treated cells demonstrated a more significant dose-dependent increase in cell death in the presence of LCL161 compared to VSVΔ51-GFP (Figure 4B). Similarly, the inclusion of LCL161 with conditioned media isolated from infected splenocytes showed a dose-dependent response in EMT6 cells (Figure 4C); however, the synergistic effect was less potent than with conditioned media derived from cancer cells, likely as a result of a lower infectivity rate of splenocytes.

We observed SMCs sensitize cancer cells to caspase-8-dependent apoptosis when infected with TNF-α-armed OVs. Notably, VSVΔ51 infection leads to the production of these cytokines in an IFNβ-dependent fashion. To confirm that TNF-α is one of the death-inducing factors from infection by VSVΔ51-TNF-α or VSVΔ51-SA:TNF-α, we downregulated TNF receptor (TNF-R1) and death receptor 5 (DR5) by siRNA transfection. The removal of TNF-R1 and DR5 resulted in loss of synergy between LCL161 and VSVΔ51-GFP in SNB75 cells (Figure 4D; Figure S6B), confirming that TNF-α and TRAIL are indispensable for bystander cell death. Surprisingly, the downregulation of both TNF-R1 and DR5 did not rescue SNB75 cell death upon LCL161 treatment and infection with VSVΔ51-TNF-α or VSVΔ51-SA:TNF-α. Consistent with these results, the incorporation of TNF-α-blocking antibodies did not rescue cell death in EMT6 cells treated with LCL161 and VSVΔ51-TNF-α or VSVΔ51-SA:TNF-α (Figure 4E). Collectively, these results suggest that there are additional components that are involved in the death of cancer cells with the combination of SMC and TNF-α-armed OVs.

A Combination of SMC and TNF-α-Armed VSV Leads to Durable Cures in Mouse Models of Cancer

We previously demonstrated that OV and SMC co-therapy is a safe and efficacious approach for the treatment of cancer in animal models.[8] The co-therapy required several rounds of treatment to achieve significant reduction of tumor growth rate and extension of mouse survival. We first assessed whether the combination is efficacious with a single treatment in the refractory orthotopic mouse model of mammary cancer, EMT6. Treatment with LCL161 as a monotherapy or in combination with VSVΔ51-GFP did not significantly slow EMT6 tumor growth (Figure 5A); however, tumor growth was significantly impaired with the inclusion of VSVΔ-TNF-α. While we observed more pronounced delay of EMT6 tumor growth in LCL161 and VSVΔ-TNF-α compared to LCL161 and VSVΔ-GFP, the difference was not statistically significant ($p = 0.20$).

For subsequent studies, we administered 50-fold less of OV compared to our previous study with less treatments[8] and limited OV treatments within 1 week to limit antibody-based neutralization of administered viruses. We first examined the efficacy of the combination in the CT-26 colon cancer tumor model, which is refractory to SMC and VSVΔ51 co-therapy. The treatment of mice bearing subcutaneous CT-26 tumors with either LCL161 or VSVΔ51-SA:TNF-α did not significantly impair the tumor growth rate nor extended mouse survival (Figure 5B). In contrast, combined LCL161 and VSVΔ51-SA:TNF-α treatment significantly induced tumor regression and an extension of mouse survival. In the orthotopic EMT6 mammary fat pad model, we observed a similar lack of efficacy with monotherapy (Figures 5C and 5D). However, consistent with the *in vitro* results, the combination of LCL161 with VSVΔ51-TNF-α or VSVΔ51-SA:TNF-α significantly attenuated tumor growth and lead to an extension of mouse survival, leading to a cure rate of 30% and 70%, respectively.

Figure 3. SMC Cotreatment with TNF-α-Armed Oncolytic VSV Induces Rapid Death of Cancer Cells

(A) Alamar blue viability assays of GM38, EMT6, and SNB75 cells treated with vehicle or 5 μM of the SMC LCL161 and increasing MOI of the indicated virus for 48 hr. Mean, SD. (B) Micrographs and quantification of DEVD-FITC signals from EMT6 and SNB75 cells treated with vehicle or 5 μM LCL161 and 1 MOI of the indicated virus. Scale bars, 50 μm. Mean, SEM. (C) SNB75 cells were transfected with non-targeting (NT), RIP1, or CASP8 siRNA for 48 hr and subsequently treated with vehicle or 5 μM LCL161 and BSA, 0.1 ng/mL TNF-α, or infected with 0.1 MOI of the indicated virus. Mean, SD.

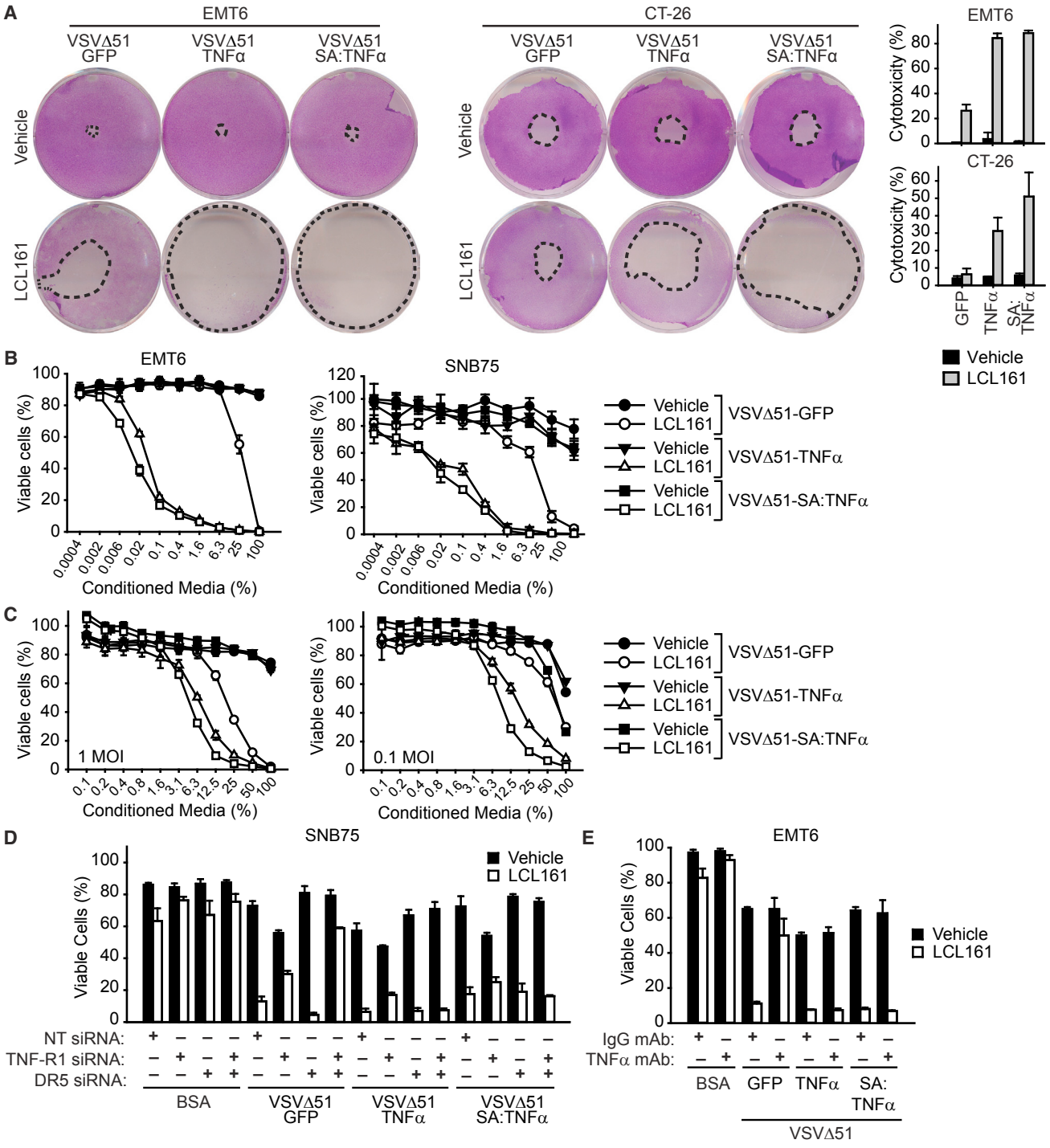

Figure 4. Infection of TNF-α-Armed Oncolytic VSV Induces Bystander Cell Death of SMC-Treated Cancer Cells

(A) Confluent monolayers of EMT6 and CT-26 cell were overlaid with agarose media containing vehicle or 5 μM of the SMC LCL161 and inoculated with 500 PFU of virus in the middle of the well for 48 hr. Cytotoxicity was assessed by crystal violet. Graph represents the percentage cytotoxicity (mean, SD). B, EMT6 and SNB75 cells were infected with 1 MOI of the indicated virus for 24 hr. The supernatant was exposed to UV light, and then the supernatant was applied at the indicated dilutions to new EMT6 or SNB75

(legend continued on next page)

Combination Treatment Leads to Vascular Shutdown and Tumor Cell Death

A previous report demonstrated that VSVΔ51 is capable of inducing vascular collapse via clot formation and endothelial cell death in CT-26 tumors.[37] Not only does TNF-α have the ability to induce apoptosis of cancer cells and tumor endothelial cells through TNF-R1 signaling, but TNF-α can also induce the secretion of blood clotting and adhesion proteins in vascular endothelium, resulting in necrosis of the tumor tissue.[38] The administration of exogenous TNF-α has been shown to be toxic to the developing neovasculature.[21,22,39] We thus sought to determine whether VSVΔ51-TNF-α infection inhibits blood flow within EMT6 tumors in the presence of SMCs. Tumor-bearing mice were injected with fluorescent microspheres to observe perfusion of these beads through the vascular system within tumors. Surprisingly, VSVΔ51-SA:TNF-α monotherapy did not significantly restrict perfusion of beads into the tumor (Figures 6A and 6B). In contrast, LCL161 monotherapy significantly reduced tumor perfusion and the inclusion of VSVΔ51-SA:TNF-α completely abrogated perfusion of these beads, although this was not statistically different from LCL161 treatment alone ($p = 0.079$). Moreover, we observed a pronounced lack of endothelial cells within the interior of the tumor in doubly treated mice (Figure 6C), suggesting that there is a complete collapse of the neovasculature within the tumor following combination treatment.

To correlate the collapse of the tumor vasculature with tumor cell death, we stained tumor sections for cleaved caspase-3. We observed an inverse relationship with the level of bead perfusion (Figures 6A and 6B) and proportion of cells positive for cleaved caspase-3 (Figures 6D and 6E) in mice treated with combinations of LCL161 and VSVΔ51-SA:TNF-α. These results confirm that there is pronounced death of tumor cells with the combination treatment.

DISCUSSION

The combination of SMCs with immunotherapies have demonstrated significant therapeutic benefits in preclinical tumor models and, consequently, these strategies are highly promising approaches to treat cancer in patients.[10,11,40–42] Here, we show that the therapeutic anti-cancer effects of the SMC LCL161 is enhanced when combined with an OV that expresses the proinflammatory cytokine TNF-α.

There are several strategies to improve the potency of oncolytic virotherapy, including those that involve the engineering of viruses to express cytokines.[25,29,31,43,44] More recently, several viral-based strategies to deliver proinflammatory cytokines, such as TNF-α, have been devised for the treatment of cancer.[21,22] A TNF-α-armed adenovirus can elicit a strong immunogenic response and induce apoptosis in B16-OVA tumors, leading to delayed tumor growth.[21] In contrast to these results, we find that the inclusion of TNF-α with oncolytic VSV is insufficient to induce tumor death in highly refractory mouse tumor models. In addition, we demonstrate that virally expressed TNF-α synergizes with LCL161, resulting in durable cures. Notably, this synergy is significant, as the extension of mouse survival and yielding of durable cures was accomplished with a log lower dose of OV and with fewer treatments compared to our previous approach.[8] Furthermore, our results are consistent with a previous report where the combination of a TNF-α-expressing adeno-associated virus bacteriophage synergizes with SMCs, resulting in prolonged survival in a xenograft melanoma model.[22]

The regulation of TNF-α-mediated signaling by the two fungible cIAPs, cIAP1 and cIAP2, is critical for vasculature maintenance. Tumor vascular collapse can be induced by IAP antagonism via TNF-α-mediated endothelial cell apoptosis.[39] Mutational inactivation of the sole cIAP member in zebrafish leads to endothelial cell sensitization to TNF-α and vascular leakage, giving rise to the hemorrhaging 'tomato' phenotype.[45] The dual genetic ablation of cIAP1 and cIAP2 in mice leads to embryonic lethality due to TNF-α toxic effects against the vasculature and potentially other tissues, which is partially rescued when the death effectors RIP1 and RIP3 are removed.[46] We found that EMT6 tumors treated with SMC alone induced significant tumor vascular collapse. This can be attributed to the fact that SMCs can induce the systemic production of TNF-α as a consequence of activating the alternative NF-κB pathway.[10] In contrast, we discovered that tumor collapse was not as pronounced with infection by TNF-α-armed oncolytic VSV alone. This finding is contrary to a study whereby VSVΔ51 infection was shown to induce vascular shutdown in CT-26 tumors.[37] The contradictory findings can be attributed toward the highly refractory nature of EMT6 tumors, which are not easily infected by VSVΔ51,[8] or by the different tumor milieu. Despite the induction of tumor vascular collapse with LCL161 or TNF-α-armed VSV monotherapy, we only observed enhanced cell death with the combination of LCL161 and TNF-α-armed VSVΔ51. Future studies are required to delineate whether multiple rounds of combinatorial treatment would lead to persistent vascular collapse and greater degree of tumor cell death. All together, this synergism can be attributed toward a dual-pronged mechanism of cell death—the stress on tumor cells as a result of transient vascular collapse and the induction of bystander cell death in the presence of SMC and elevated levels of TNF-α.

We observed synergistic effects with the combination of LCL161 and either systematically or locally delivered TNF-α-armed VSVΔ51. The expression of TNF-α in infected non-tumor-bearing mice and the pronounced efficacy with systematic injection of TNF-α-armed OVs suggests that local production of TNF-α within the tumor milieu is not absolutely required for synergy. This result is in agreement with our previous finding that the combination of SMCs and OVs induces

cells in the presence of vehicle or 5 μM LCL161 for 48 hr. (C) Conditioned media from splenocytes was generated as in (B) and applied to EMT6 cells in the presence of vehicle or 5 μM LCL161 for 48 hr. (D) SNB75 cells were transfected with combinations of nontargeting (NT), TNF-R1, and DR5 siRNA for 48 hr and treated with vehicle or 5 μM LCL161 and infected with the indicated virus for 48 hr. (E) EMT6 cells were pretreated with 50 μg/mL of TNF-α neutralizing antibody or isotype IgG control for 1 hr and subsequently treated with 5 μM LCL161 and 1 MOI of the indicated virus. (B–E) Cell viability was assessed by Alamar blue. Mean, SD.

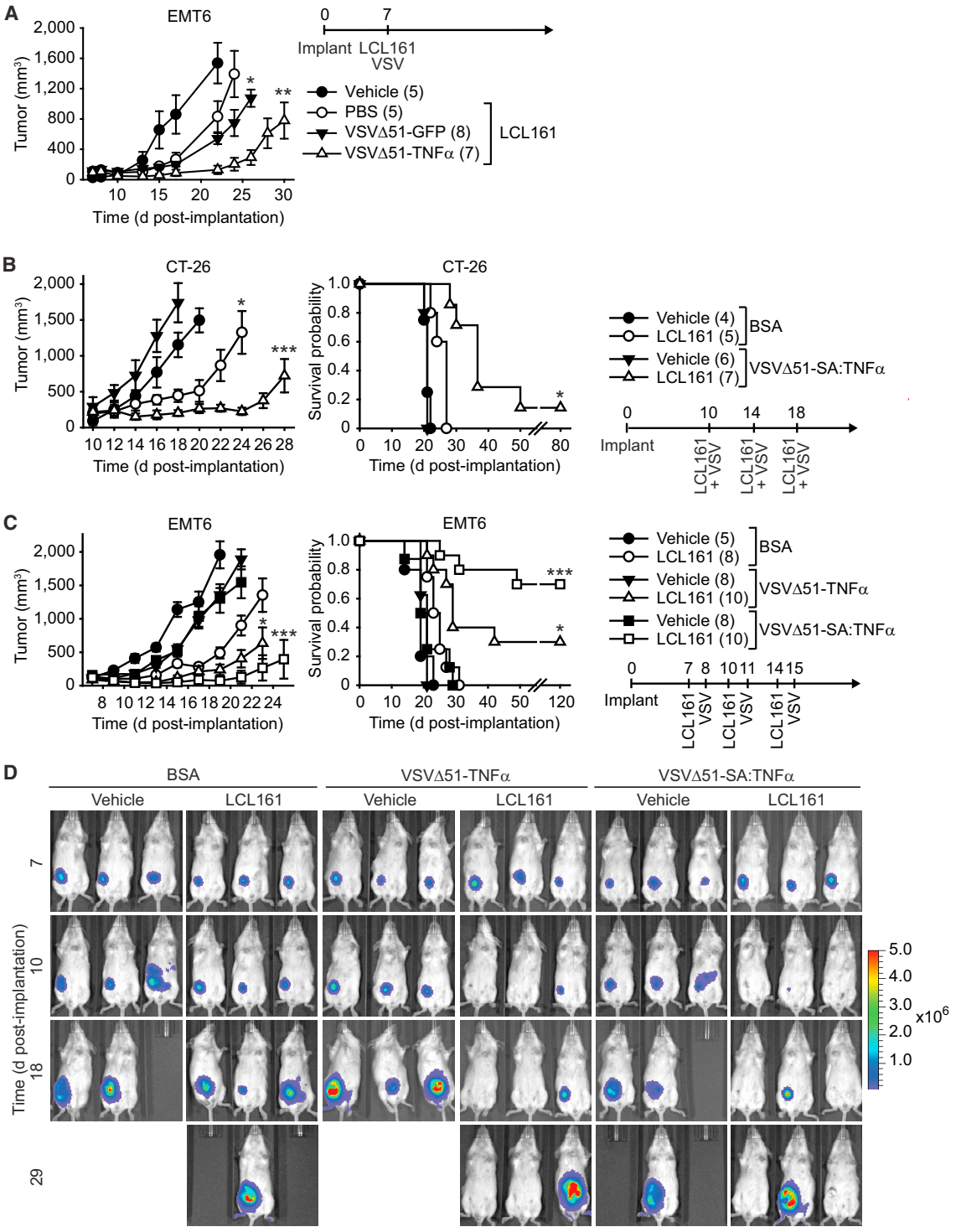

Figure 5. TNF-α-Armed Oncolytic VSV Potently Synergize with SMC *In Vivo*

(A) Mice with established ~100 mm^3 mammary tumors were treated with vehicle or 50 mg/kg of the SMC LCL161 (oral gavage) and 1×10^7 PFU of VSVΔ51-GFP or VSVΔ51-TNF-α (intravenous). (B) Mice bearing ~200 mm^3 CT-26 tumors were treated with vehicle or 50 mg/kg LCL161 (oral gavage) and 1×10^7 PFU of VSVΔ51-SA:TNF-α intratumorally. (C) Mice bearing ~100 mm^3 EMT6-Fluc tumors were treated with vehicle or 50 mg/kg of LCL161 (oral gavage) and 1×10^7 PFU of VSVΔ51-TNF-α or

(legend continued on next page)

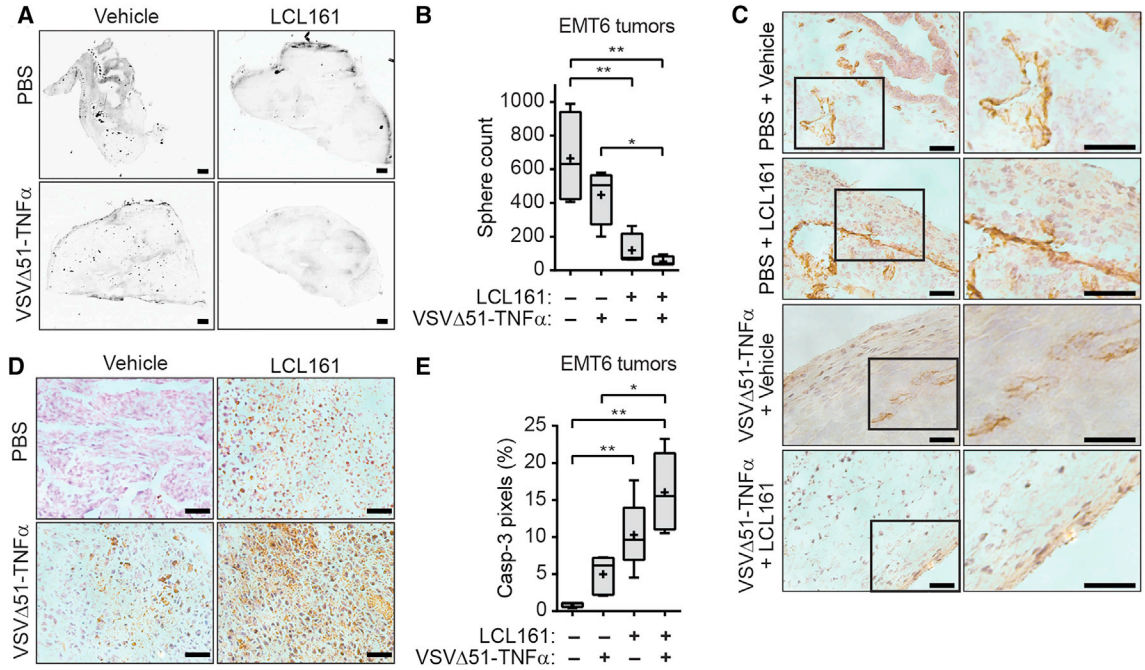

Figure 6. Combination Treatment of SMC and TNF-α-Armed Oncolytic VSV Induces Vascular Shutdown and Tumor Cell Death

(A) EMT6-bearing mice were treated with vehicle or 50 mg/kg of the SMC LCL161 orally and PBS or 1×10^7 PFU of VSVΔ51-TNF-α intratumorally for 24 hr and injected with fluorescent microspheres (i.v.) for 5 min. Tumor sections were scanned using the Agilent Technologies DNA microarray scanner. Scale bar, 200 μm. (B) Quantification of perfused microspheres described in (A). One-way ANOVA, *p < 0.05. (C) Tumor sections from the experiment depicted in (A) were stained with anti-CD31 and counterstained with hematoxylin. Scale bars, 50 μm. (D) Immunohistochemistry of tumor sections from (A) stained for cleaved CASP3. Scale bars, 50 μm. (E) Quantification of the percentage of caspase-3 pixels. One-way ANOVA, *p < 0.05; **p < 0.01. Mean, SD. Crosses, mean; solid horizontal lines, median; boxes, 25th to 75th percentile; whiskers, min–max range of the values.

tumor regression through a bystander cell-death mechanism.[8] While we did not observe overt toxicity with the combination of LCL161 and VSVΔ51-TNF-α administered intravenously (i.v.), a local injection of these cytokine-armed viruses may represent a more clinically relevant platform for delivery, as we observed striking synergy in tested refractory cancer models. For instance, intratumoral injection of VSV-IFNβ is currently being tested in a phase I clinical trial for patients with liver tumors (NCT01628640). However, further studies are required to determine the specific origin and/or requirement of local versus systematic TNF-α, the contribution of infected tumor or non-tumor cells (e.g., stromal cells, epithelial cells, immune cells), and whether co-therapy of a systemic or local administration of these viruses is required for maximal eradication of disseminated or metastatic tumors.

In summary, we report the generation of novel TNF-α-secreting OVs based on the VSVΔ51 backbone, which are superior to VSVΔ51 at inducing LCL161-mediated cancer cell death. The TNF-α viruses were shown to have similar potency *in vitro*; however, the inclusion of the secretory sequence in VSVΔ51-SA:TNF-α resulted in a stronger synergistic response to LCL161 treatment *in vivo* compared to VSVΔ51-TNF-α. This approach was found to be safe and efficacious in mice bearing aggressive, syngeneic tumors. In addition, fewer treatments were necessary to achieve improved responses when compared to *in vivo* experiments performed with VSVΔ51 and LCL161. Together, this data demonstrates that the therapeutic efficacy of SMC is greatly enhanced when used in combination with the exogenous delivery of TNF-α. Given the results produced in this study, we believe that SMC and TNF-α-armed OVs could potentially be used as a new, highly efficacious form of combination immunotherapy for cancer treatment.

MATERIALS AND METHODS

Cell Culture

EMT6, CT-26, 786-0, GM38, H460, H661, and Vero cells were obtained from ATCC, SNB75 cells was provided by the National Cancer Institute (NIH), and SF539 was acquired from UCSF Brain Tumor Bank. Cells were maintained at 37°C and 5% CO_2 in DMEM media

VSVΔ51-SA:TNF-α (intratumoral). (D) IVIS images of representative EMT6-Fluc-bearing mice described in (B). Scale, p/s/cm^2/sr (photons per second per square centimeter per steradian). (A–C) Left panel depicts tumor growth (mean, SEM); right panel represents the Kaplan-Meier curve depicting mouse survival. Statistical significance of tumor growth rates was assessed by one-way ANOVA with Tukey's multiple comparison. Log rank with Holm-Sidak multiple comparison: *p < 0.05; **p < 0.01; ***p < 0.001. Number of mice per treatment group is displayed in brackets.

supplemented with 10% heat-inactivated fetal calf serum (FCS) and 1% non-essential amino acids (Invitrogen). The cell lines were authenticated by the providers. Cell lines were tested for mycoplasma contamination twice a year (Universal Mycoplasma Detection Kit, ATCC). Splenocytes were isolated from 8-week-old female BALB/c mice and maintained in RPMI media with 10% fetal calf serum (FCS) and 50 μM β-mercaptoethanol.

Recombinant Viruses

The Indiana serotype of VSVΔ51 was used in this study and was propagated in Vero cells. VSVΔ51-TNF-α was generated by cloning the full-length human TNF-α sequence between the glycoprotein (G) and polymerase (L) viral genes. Similarly, VSVΔ51-SA:TNF-α was constructed by replacing the membrane anchor domain with the human serum albumin (SA) signal peptide sequence. VSVΔ51-GFP is a recombinant derivative of VSVΔ51 expressing jellyfish GFP. VSVΔ51-Fluc is a recombinant derivative of VSVΔ51 expressing firefly luciferase. All VSVΔ51 constructs were purified on an OptiPrep gradient (Sigma). Viral titer was determined by standard plaque assays using Vero cells. Multistep growth curves were determined by adding serially diluted supernatants to Vero cells for 3 days. The cells were then fixed and stained with crystal violet and scored for dead wells in order to calculate the 50% tissue culture infective dose ($TCID_{50}$).

Viability Assays

Cells were treated with vehicle (0.05% DMSO) or 5 μM of the SMC LCL161 (provided by Novartis)[47] and infected with the indicated MOI. Cell viability was determined by Alamar blue (Sigma), and data were normalized to vehicle treatment. To measure the rate of cell death, 1 μM DEVD-488 (Essen Bioscience) was added to cells, and images were acquired using the IncuCyte Zoom live microscope. Enumeration of fluorescence signals was processed using the integrated object counting algorithm within the IncuCyte Zoom software.

ELISA

Supernatants were collected from cells treated with vehicle or LCL161 and infected with indicated MOI. Cytokines were measured using the TNF-α DuoSet ELISA kit (R&D Systems) or Verikine IFNβ ELISA Kit (PBL Interferon Source). Serum was collected from 5-week-old BALB/c mice infected with 1×10^8 plaque forming units (PFU) virus, and TNF-α levels were measured using the TNF-α Quantikine high-sensitivity assay kit (R&D Systems).

Virus Spreading and Conditioned Media Transfer Assays

For the virus-spreading assay, cells were overlaid with 1% agarose in DMEM complete media. Subsequently, a hole was punched in the middle of the well, cells were inoculated with 500 PFU of the indicated virus and overlaid with vehicle or 5 μM LCL161 for 48 hr. Cells were fixed with 3:1 mixture of methanol:acetic acid and stained with crystal violet. For the conditioned media transfer assay, cells were infected with indicated MOI of OV for 24 hr, and the infectious virions were inactivated by exposure to UV light. The supernatant was subsequently applied to cells in the presence of vehicle or 5 μM LCL161. Cell viability was assessed by Alamar blue.

siRNA-Mediated Knockdown and Antibody Neutralization

Cells were transfected with combinations of non-targeting (NT), Receptor Interacting Protein1 (RIP1), Caspase-8 (CASP8), TNF-R1, and DR5 small interfering RNA (siRNA) (ON-Target SmartPool, Thermo Fisher Scientific) for 48 hr. Cells were then treated with vehicle or 5 μM LCL161 and infected with the indicated OV. Cell viability was assessed by Alamar blue. Knockdown of TNF-R1 and DR5 was determined by western blotting using the following antibodies: RIP1 (D94C12; Cell Signaling Technology), CASP8 (AF705), DR5 (3696; Cell Signaling Technology), TNF-R1 (3736; Cell Signaling Technology), β-tubulin (E7; Developmental Studies Hybridoma Bank), and GAPDH (GAPDH-71.1; Sigma). For antibody-mediated neutralization of TNF-α, cells were treated with 50 μg/mL of mouse immunoglobulin G (IgG) control (HRPN; BioXCell) or anti-TNF-α (XT3.11; BioXCell). One hour later, cells were treated with vehicle or 5 μM LCL161 and the indicated MOI of OV. Cell viability was assessed by Alamar blue.

Animal Tumor Studies

All animal study protocols were performed under approval of the University of Ottawa's Animal Care and Veterinarian Services committee. Mammary tumors were established by injecting 1×10^5 EMT6 cells in the mammary fat pad of 5-week-old female BALB/c mice. Subcutaneous CT-26 colon cancer models were established by injecting mice with 3×10^5 cells in the right hind-flank. Mice with palpable tumors were co-treated with either vehicle (30% 0.1 M HCl, 70% 0.1 M NaOAc [pH 4.63]) or 50 mg/kg LCL161 orally and injections of PBS or oncolytic VSV. Tumor volume was calculated using the formula $(\pi)(W)^2(L)/4$, where W = tumor width and L = tumor length. Animals were euthanized when the tumor burden exceeded 2,000 mm^3.

For the analysis of tumor vascular collapse, EMT6-bearing mice were treated with vehicle or 50 mg/kg LCL161 and 1×10^8 PFU VSVΔ51-TNF-α 15 days post-implantation. The next day, the mice were injected i.v. with a 50:50 solution of 100 nm diameter orange fluorescent microspheres in PBS (Molecular Probes). Five minutes later, mice were euthanized and the excised tumors were snap frozen in OCT compound. Tumors were cut into 10-μm sections, and beads were visualized by a DNA Microarray Scanner (Agilent Technologies) using the red laser. For immunohistochemistry, tumors were fixed in 4% paraformaldehyde overnight and embedded in a 1:1 mixture of OCT and 30% sucrose. Tumors were sectioned at 12 μm, stained with cleaved caspase-3 (9661; Cell Signaling Technologies), and colorimetric development was used using the Vectastain system (Vector Laboratories). Alternatively, tumors were fixed in a mixture of 75% acetone and 25% ethanol for 5 min at 4°C and embedded in OCT. Tissues were sectioned at 10 μm and stained with anti-CD31 (ab28364; Abcam) using the Vectastain system. ImageJ was used for quantitation of spheres or cleaved caspase-3.

Statistical Analysis

Statistical analysis for quantification of microspheres/area and cleaved caspase-3 was performed using non-parametric ANOVA. Statistical significance of tumor growth rates (by calculating the slope derived from log-transformed tumor volumes over time) was determined using one-way ANOVA with Tukey's multiple comparison. Log rank with Holm-Sidak multiple comparison was performed for Kaplan-Meier curves depicting mouse survival.

SUPPLEMENTAL INFORMATION

Supplemental Information includes six figures and can be found with this article online at https://doi.org/10.1016/j.omto.2018.06.002.

AUTHOR CONTRIBUTIONS

S.T.B. and S.J.P. designed the experiments. S.T.B., S.J.P., M.S.-J., J.H., and D.E.W. conducted the experiments. S.T.B., S.J.P., E.C.L., and R.G.K. wrote the paper.

ACKNOWLEDGMENTS

We acknowledge the help and advice of Dr. Naomi Da Silva (OHRI, Bell Laboratory). We thank Dr. Alexandre Blais for the use of the DNA microarray scanner. This paper is dedicated to the late Dr. D.P. Thornhill (Health Canada, Ottawa). This work was supported by an Impact grant co-funded by the Canadian Cancer Society Research Institute (CCSRI) and Brain Canada (704119) and operating grants from the Canadian Institutes of Health Research (231421, 318176, and 361847 to R.G.K., S.T.B., and E.C.L.) and funding from the Ottawa Regional Cancer Foundation (ORCF), including funds from the Ottawa Kiwanis Medical Foundation (to R.G.K.) .

REFERENCES

1. Fulda, S., and Vucic, D. (2012). Targeting IAP proteins for therapeutic intervention in cancer. Nat. Rev. Drug Discov. *11*, 109–124.
2. Fulda, S. (2015). Promises and Challenges of Smac Mimetics as Cancer Therapeutics. Clin. Cancer Res. *21*, 5030–5036.
3. Mahoney, D.J., Cheung, H.H., Mrad, R.L., Plenchette, S., Simard, C., Enwere, E., Arora, V., Mak, T.W., Lacasse, E.C., Waring, J., and Korneluk, R.G. (2008). Both cIAP1 and cIAP2 regulate TNFalpha-mediated NF-kappaB activation. Proc. Natl. Acad. Sci. USA *105*, 11778–11783.
4. Hunter, A.M., LaCasse, E.C., and Korneluk, R.G. (2007). The inhibitors of apoptosis (IAPs) as cancer targets. Apoptosis *12*, 1543–1568.
5. Ea, C.K., Deng, L., Xia, Z.P., Pineda, G., and Chen, Z.J. (2006). Activation of IKK by TNFalpha requires site-specific ubiquitination of RIP1 and polyubiquitin binding by NEMO. Mol. Cell *22*, 245–257.
6. Wu, C.J., Conze, D.B., Li, T., Srinivasula, S.M., and Ashwell, J.D. (2006). Sensing of Lys 63-linked polyubiquitination by NEMO is a key event in NF-kappaB activation [corrected]. Nat. Cell Biol. *8*, 398–406.
7. Blankenship, J.W., Varfolomeev, E., Goncharov, T., Fedorova, A.V., Kirkpatrick, D.S., Izrael-Tomasevic, A., Phu, L., Arnott, D., Aghajan, M., Zobel, K., et al. (2009). Ubiquitin binding modulates IAP antagonist-stimulated proteasomal degradation of c-IAP1 and c-IAP2(1). Biochem. J. *417*, 149–160.
8. Beug, S.T., Tang, V.A., LaCasse, E.C., Cheung, H.H., Beauregard, C.E., Brun, J., Nuyens, J.P., Earl, N., St-Jean, M., Holbrook, J., et al. (2014). Smac mimetics and innate immune stimuli synergize to promote tumor death. Nat. Biotechnol. *32*, 182–190.
9. Cheung, H.H., Beug, S.T., St Jean, M., Brewster, A., Kelly, N.L., Wang, S., and Korneluk, R.G. (2010). Smac mimetic compounds potentiate interleukin-1beta-mediated cell death. J. Biol. Chem. *285*, 40612–40623.
10. Beug, S.T., Beauregard, C.E., Healy, C., Sanda, T., St-Jean, M., Chabot, J., Walker, D.E., Mohan, A., Earl, N., Lun, X., et al. (2017). Smac mimetics synergize with immune checkpoint inhibitors to promote tumour immunity against glioblastoma. Nat. Commun. *8*, 14278.
11. Chesi, M., Mirza, N.N., Garbitt, V.M., Sharik, M.E., Dueck, A.C., Asmann, Y.W., Akhmetzyanova, I., Kosiorek, H.E., Calcinotto, A., Riggs, D.L., et al. (2016). IAP antagonists induce anti-tumor immunity in multiple myeloma. Nat. Med. *22*, 1411–1420.
12. Roberts, N.J., Zhou, S., Diaz, L.A., Jr., and Holdhoff, M. (2011). Systemic use of tumor necrosis factor alpha as an anticancer agent. Oncotarget *2*, 739–751.
13. Balkwill, F. (2009). Tumour necrosis factor and cancer. Nat. Rev. Cancer *9*, 361–371.
14. Asher, A., Mule, J.J., Reichert, C.M., Shiloni, E., and Rosenberg, S.A. (1987). Studies on the anti-tumor efficacy of systemically administered recombinant tumor necrosis factor against several murine tumors in vivo. J. Immunol. *138*, 963–974.
15. Salmon, S.E., Young, L., Scuderi, P., and Clark, B. (1987). Antineoplastic effects of tumor necrosis factor alone and in combination with gamma-interferon on tumor biopsies in clonogenic assay. J. Clin. Oncol. *5*, 1816–1821.
16. Gamm, H., Lindemann, A., Mertelsmann, R., and Herrmann, F. (1991). Phase I trial of recombinant human tumour necrosis factor alpha in patients with advanced malignancy. Eur. J. Cancer *27*, 856–863.
17. Creaven, P.J., Brenner, D.E., Cowens, J.W., Huben, R.P., Wolf, R.M., Takita, H., Arbuck, S.G., Razack, M.S., and Proefrock, A.D. (1989). A phase I clinical trial of recombinant human tumor necrosis factor given daily for five days. Cancer Chemother. Pharmacol. *23*, 186–191.
18. Hoekstra, H.J., Veerman, K., and van Ginkel, R.J. (2014). Isolated limb perfusion for in-transit melanoma metastases: melphalan or TNF-melphalan perfusion? J. Surg. Oncol. *109*, 338–347.
19. Taeger, G., Grabellus, F., Podleska, L.E., Muller, S., and Ruchholtz, S. (2008). Effectiveness of regional chemotherapy with TNF-alpha/melphalan in advanced soft tissue sarcoma of the extremities. Int. J. Hyperthermia *24*, 193–203.
20. Deroose, J.P., Eggermont, A.M., van Geel, A.N., de Wilt, J.H., Burger, J.W., and Verhoef, C. (2012). 20 years experience of TNF-based isolated limb perfusion for in-transit melanoma metastases: TNF-dose matters. Ann. Surg. Oncol. *19*, 627–635.
21. Hirvinen, M., Rajecki, M., Kapanen, M., Parviainen, S., Rouvinen-Lagerström, N., Diaconu, I., Nokisalmi, P., Tenhunen, M., Hemminki, A., and Cerullo, V. (2015). Immunological effects of a tumor necrosis factor alpha-armed oncolytic adenovirus. Hum. Gene Ther. *26*, 134–144.
22. Yuan, Z., Syrkin, G., Adem, A., Geha, R., Pastoriza, J., Vrikshajanani, C., Smith, T., Quinn, T.J., Alemu, G., Cho, H., et al. (2013). Blockade of inhibitors of apoptosis (IAPs) in combination with tumor-targeted delivery of tumor necrosis factor-α leads to synergistic antitumor activity. Cancer Gene Ther. *20*, 46–56.
23. Stojdl, D.F., Lichty, B.D., tenOever, B.R., Paterson, J.M., Power, A.T., Knowles, S., Marius, R., Reynard, J., Poliquin, L., Atkins, H., et al. (2003). VSV strains with defects in their ability to shutdown innate immunity are potent systemic anti-cancer agents. Cancer Cell *4*, 263–275.
24. Lichty, B.D., Breitbach, C.J., Stojdl, D.F., and Bell, J.C. (2014). Going viral with cancer immunotherapy. Nat. Rev. Cancer *14*, 559–567.
25. Kurisetty, V.V.S., Heiber, J., Myers, R., Pereira, G.S., Goodwin, J.W., Federspiel, M.J., Russell, S.J., Peng, K.W., Barber, G., and Merchan, J.R. (2014). Preclinical safety and activity of recombinant VSV-IFN-β in an immunocompetent model of squamous cell carcinoma of the head and neck. Head Neck *36*, 1619–1627.
26. Zhang, L., Steele, M.B., Jenks, N., Grell, J., Suksanpaisan, L., Naik, S., Federspiel, M.J., Lacy, M.Q., Russell, S.J., and Peng, K.W. (2016). Safety Studies in Tumor and Non-Tumor-Bearing Mice in Support of Clinical Trials Using Oncolytic VSV-IFNβ-NIS. Hum. Gene Ther. Clin. Dev. *27*, 111–122.
27. Lemay, C.G., Rintoul, J.L., Kus, A., Paterson, J.M., Garcia, V., Falls, T.J., Ferreira, L., Bridle, B.W., Conrad, D.P., Tang, V.A., et al. (2012). Harnessing oncolytic virus-mediated antitumor immunity in an infected cell vaccine. Mol. Ther. *20*, 1791–1799.

28. Bourgeois-Daigneault, M.C., Roy, D.G., Falls, T., Twumasi-Boateng, K., St-Germain, L.E., Marguerie, M., Garcia, V., Selman, M., Jennings, V.A., Pettigrew, J., et al. (2016). Oncolytic vesicular stomatitis virus expressing interferon-γ has enhanced therapeutic activity. Mol. Ther. Oncolytics *3*, 16001.

29. Stephenson, K.B., Barra, N.G., Davies, E., Ashkar, A.A., and Lichty, B.D. (2012). Expressing human interleukin-15 from oncolytic vesicular stomatitis virus improves survival in a murine metastatic colon adenocarcinoma model through the enhancement of anti-tumor immunity. Cancer Gene Ther. *19*, 238–246.

30. Shin, E.J., Wanna, G.B., Choi, B., Aguila, D., 3rd, Ebert, O., Genden, E.M., and Woo, S.L. (2007). Interleukin-12 expression enhances vesicular stomatitis virus oncolytic therapy in murine squamous cell carcinoma. Laryngoscope *117*, 210–214.

31. Naik, S., Nace, R., Federspiel, M.J., Barber, G.N., Peng, K.W., and Russell, S.J. (2012). Curative one-shot systemic virotherapy in murine myeloma. Leukemia *26*, 1870–1878.

32. Willmon, C.L., Saloura, V., Fridlender, Z.G., Wongthida, P., Diaz, R.M., Thompson, J., Kottke, T., Federspiel, M., Barber, G., Albelda, S.M., and Vile, R.G. (2009). Expression of IFN-beta enhances both efficacy and safety of oncolytic vesicular stomatitis virus for therapy of mesothelioma. Cancer Res. *69*, 7713–7720.

33. Vandenabeele, P., and Bertrand, M.J. (2012). The role of the IAP E3 ubiquitin ligases in regulating pattern-recognition receptor signalling. Nat. Rev. Immunol. *12*, 833–844.

34. Beug, S.T., Cheung, H.H., LaCasse, E.C., and Korneluk, R.G. (2012). Modulation of immune signalling by inhibitors of apoptosis. Trends Immunol. *33*, 535–545.

35. Cheung, H.H., Mahoney, D.J., Lacasse, E.C., and Korneluk, R.G. (2009). Down-regulation of c-FLIP Enhances death of cancer cells by smac mimetic compound. Cancer Res. *69*, 7729–7738.

36. Melcher, A., Parato, K., Rooney, C.M., and Bell, J.C. (2011). Thunder and lightning: immunotherapy and oncolytic viruses collide. Mol. Ther. *19*, 1008–1016.

37. Breitbach, C.J., De Silva, N.S., Falls, T.J., Aladl, U., Evgin, L., Paterson, J., Sun, Y.Y., Roy, D.G., Rintoul, J.L., Daneshmand, M., et al. (2011). Targeting tumor vasculature with an oncolytic virus. Mol. Ther. *19*, 886–894.

38. van Horssen, R., Ten Hagen, T.L., and Eggermont, A.M. (2006). TNF-alpha in cancer treatment: molecular insights, antitumor effects, and clinical utility. Oncologist *11*, 397–408.

39. Witt, A., Seeger, J.M., Coutelle, O., Zigrino, P., Broxtermann, P., Andree, M., Brinkmann, K., Jüngst, C., Schauss, A.C., Schüll, S., et al. (2015). IAP antagonization promotes inflammatory destruction of vascular endothelium. EMBO Rep. *16*, 719–727.

40. Oost, T.K., Sun, C., Armstrong, R.C., Al-Assaad, A.S., Betz, S.F., Deckwerth, T.L., Ding, H., Elmore, S.W., Meadows, R.P., Olejniczak, E.T., et al. (2004). Discovery of potent antagonists of the antiapoptotic protein XIAP for the treatment of cancer. J. Med. Chem. *47*, 4417–4426.

41. Sun, H., Nikolovska-Coleska, Z., Lu, J., Qiu, S., Yang, C.Y., Gao, W., Meagher, J., Stuckey, J., and Wang, S. (2006). Design, synthesis, and evaluation of a potent, cell-permeable, conformationally constrained second mitochondria derived activator of caspase (Smac) mimetic. J. Med. Chem. *49*, 7916–7920.

42. Houghton, P.J., Kang, M.H., Reynolds, C.P., Morton, C.L., Kolb, E.A., Gorlick, R., Keir, S.T., Carol, H., Lock, R., Maris, J.M., et al. (2012). Initial testing (stage 1) of LCL161, a SMAC mimetic, by the Pediatric Preclinical Testing Program. Pediatr. Blood Cancer *58*, 636–639.

43. Liu, Y.P., Steele, M.B., Suksanpaisan, L., Federspiel, M.J., Russell, S.J., Peng, K.W., and Bakkum-Gamez, J.N. (2014). Oncolytic measles and vesicular stomatitis virotherapy for endometrial cancer. Gynecol. Oncol. *132*, 194–202.

44. LeBlanc, A.K., Naik, S., Galyon, G.D., Jenks, N., Steele, M., Peng, K.W., Federspiel, M.J., Donnell, R., and Russell, S.J. (2013). Safety studies on intravenous administration of oncolytic recombinant vesicular stomatitis virus in purpose-bred beagle dogs. Hum. Gene Ther. Clin. Dev. *24*, 174–181.

45. Santoro, M.M., Samuel, T., Mitchell, T., Reed, J.C., and Stainier, D.Y. (2007). Birc2 (cIap1) regulates endothelial cell integrity and blood vessel homeostasis. Nat. Genet. *39*, 1397–1402.

46. Wong, W.W., Vince, J.E., Lalaoui, N., Lawlor, K.E., Chau, D., Bankovacki, A., Anderton, H., Metcalf, D., O'Reilly, L., Jost, P.J., et al. (2014). cIAPs and XIAP regulate myelopoiesis through cytokine production in an RIPK1- and RIPK3-dependent manner. Blood *123*, 2562–2572.

47. Chen, K.F., Lin, J.P., Shiau, C.W., Tai, W.T., Liu, C.Y., Yu, H.C., Chen, P.J., and Cheng, A.L. (2012). Inhibition of Bcl-2 improves effect of LCL161, a SMAC mimetic, in hepatocellular carcinoma cells. Biochem. Pharmacol. *84*, 268–277.